Hindawi Publishing Corporation
Journal of Nanomaterials
Volume 2015, Article ID 802178, 6 pages
http://dx.doi.org/10.1155/2015/802178

*Research Article*

# Controlled Orientation and Improved Photovoltaic Characteristics of $Cu(In,Ga)Se_2$ Solar Cells via Using $In_2Se_3$ Seeding Layers

**Fu-Shan Chen, Che-Yuan Yang, Jen-Cheng Sung, and Chung-Hsin Lu**

*Department of Chemical Engineering, National Taiwan University, Taipei, Taiwan*

Correspondence should be addressed to Chung-Hsin Lu; chlu@ntu.edu.tw

Received 8 October 2014; Accepted 12 December 2014

Academic Editor: Victor M. Castaño

Copyright © 2015 Fu-Shan Chen et al. This is an open access article distributed under the Creative Commons Attribution License, which permits unrestricted use, distribution, and reproduction in any medium, provided the original work is properly cited.

$In_2Se_3$ films were utilized as seeding layers in the synthesis of $Cu(In,Ga)Se_2$ films via the spin-coating route. Selenizing the indium-containing precursors at 400°C resulted in the formation of the hexagonal $\gamma$-$In_2Se_3$ with the preferred (006) orientation. Increasing the selenization temperature to 500°C yielded the (300)-oriented $\gamma$-$In_2Se_3$. Using the preferred (006)-oriented $In_2Se_3$ as seeding layers produced the preferred (112)-oriented $Cu(In,Ga)Se_2$ film because of the crystalline symmetry. In contrast, the use of the (300)-oriented $In_2Se_3$ as seeding layers yielded the (220/204)-oriented $Cu(In,Ga)Se_2$ films. According to results obtained using SEM and the Hall effect, (112)-oriented $Cu(In,Ga)Se_2$ films had a denser morphology and more favorable electrical properties. Using the (112)-oriented $Cu(In,Ga)Se_2$ films as the absorber layer in the solar devices resulted in a significant increase in the conversion efficiency.

## 1. Introduction

$Cu(In,Ga)Se_2$ is an important absorber material utilized in thin-film solar devices because of a high absorption coefficient and a direct band gap [1, 2]. This material exhibits a chalcopyrite structure and high-quality $Cu(In,Ga)Se_2$ is generally synthesized via a three-step evaporation process [3, 4]. The process involves firstly depositing $(In,Ga)_2Se_3$ films, followed by copper and selenium, and finally indium, gallium, and selenium to form $Cu(In,Ga)Se_2$ films [5]. The deposition of $(In,Ga)_2Se_3$ with different crystalline structures affects the orientation of the prepared $Cu(In,Ga)Se_2$ films. The condition of the deposition process influences the crystalline structures of $(In,Ga)_2Se_3$ [6–8].

$In_2Se_3$ is used as the precursors to control the orientation of $Cu(In,Ga)Se_2$ films that are prepared via other vacuum deposition processes [9]. However, the control of the orientation of $Cu(In,Ga)Se_2$ films that are formed via nonvacuum routes has not been investigated in detail. In this study, $In_2Se_3$ was prepared via the selenization process and then applied as the seeding layer for controlling the orientation of solution-based $Cu(In,Ga)Se_2$ films. Metal nitrates ware used as the starting materials in the preparation of the pastes for coating the precursor films. Therefore, the cost of process can be substantially reduced. Indium-containing precursor films can be selenized at various temperatures for controlling the orientation of the obtained seeding layer-$In_2Se_3$. The preparation of the $Cu(In,Ga)Se_2$ films via the spin-coating process using the seeding layers was investigated. The relation between the orientation of $In_2Se_3$ and the orientation of $Cu(In,Ga)Se_2$ films as well as the electrical properties was discussed. Solar cells with these absorber layers were also fabricated for investigating their device performance.

## 2. Experimental

For preparing $In_2Se_3$ seeding layers, indium (III) nitrate was used as the starting materials and dissolved in ethanol. The viscosity of the solutions was increased via adding ethyl cellulose used as a binder. The seeding layers were spin-coated on the glass substrates employing the above solution, followed by heating at 200°C on a hot plate for removing solvent and carbon species. The as-coated seeding layers were

then heated in the range of 200–500°C for 0.5 h in a reducing atmosphere (5 vol% $H_2$ and 95 vol% $N_2$) containing Se vapor. Additionally, copper (II) nitrate, indium (III) nitrate, and gallium (III) nitrate were dissolved in ethanol, and then ethyl cellulose was added as a binder. The final molar ratio of copper ions to IIIA ions for Cu(In,Ga)$Se_2$ was close to that reported in the literature [10]. The as-prepared solutions were spin-coated on the seeding layers to prepare the precursor films, and then the precursor films were heated to 200°C on a hot plate. The precursor films were later selenized at 500°C for 0.5 h for synthesizing Cu(In,Ga)$Se_2$ films.

The formed phases in the selenized films were analyzed using an X-ray diffractometer (XRD, Philips X'Pert) operated as 40 kV and 40 mA with Cu K$\alpha$ radiation. The morphology of the obtained films was examined using a scanning electron microscope (SEM, Nova NanoSEM 230). The electrical properties of the prepared films were investigated using a Hall effect measurement (HMS-3000) at room temperature.

Cu(In,Ga)$Se_2$ solar cells employing the seeding layers were fabricated for investigating solar cell parameters. CdS was deposited on Cu(In,Ga)$Se_2$ films via a chemical bath deposition method. Subsequently, intrinsic zinc oxide (i-ZnO) and tin-doped indium oxide (ITO) were deposited via the rf-magnetron sputtering. Finally, the Cu(In,Ga)$Se_2$ solar cells were characterized via the current-voltage ($I$-$V$) measurement under AM1.5G conditions at 25°C.

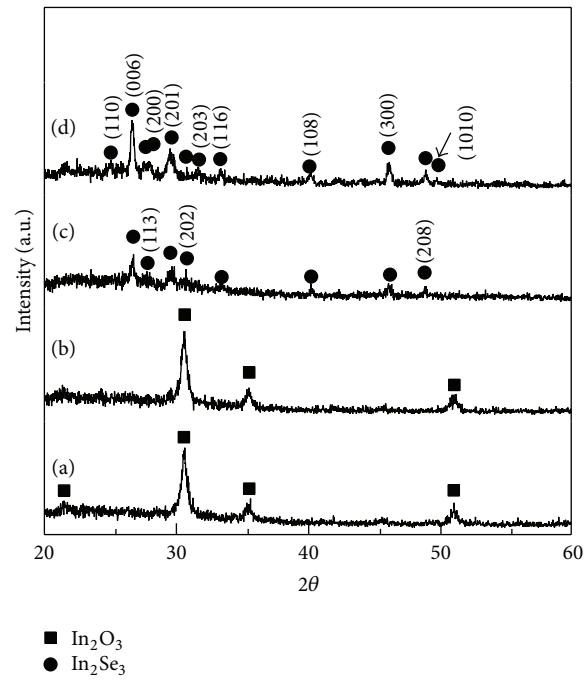


Figure 1: X-ray diffraction patterns of the seeding layers (a) without selenization and selenized at (b) 300°C, (c) 400°C, and (d) 500°C.

## 3. Results and Discussion

$In_2Se_3$ films with a thickness of 400 nm were coated on glass substrates employing indium-containing pastes and subsequently dried at 200°C. Figure 1 presents the XRD patterns of the indium-containing films that were selenized at various temperatures. Only $In_2O_3$ was identified when the indium-containing films were prepared without selenization (Figure 1(a)) and those were selenized at 300°C (Figure 1(b)). Following selenization at 400°C, the XRD patterns of the indium-containing layers closely matched the defective wurtzite structure of the hexagonal $\gamma$-$In_2Se_3$ (JCPDS number 70-0250) (Figure 1(c)). $\gamma$-$In_2Se_3$ is known to be yielded as the stable phase at 350°C [11]. Further selenizing at 500°C monotonically increased the XRD intensity of $In_2Se_3$ films. The ratios of the XRD intensity of the (006) peak to that of the (300) peak for 400°C-selenized $In_2Se_3$ films and 500°C-selenized $In_2Se_3$ films were calculated to be 2.92 and 2.37, respectively, revealing that $In_2Se_3$ films exhibited a preferred (006) orientation upon selenization at 400°C. In contrast, $In_2Se_3$ films exhibited a slightly preferred (300) orientation after further selenizing at 500°C. Hexagonal $In_2Se_3$ exhibits many phases such as $\alpha$-$In_2Se_3$ and $\beta$-$In_2Se_3$ [12, 13]. Hence, the orientation of $In_2Se_3$ films can be effected by the phase transition when the selenization process is carried out at high temperatures.

$In_2Se_3$ films that were selenized at different temperatures were applied as the seeding layers for preparing Cu(In,Ga)$Se_2$. Figure 2 presents the representative XRD patterns of the 500°C-selenized Cu(In,Ga)$Se_2$ films that were coated on the seeding layers. The XRD patterns of Cu(In,Ga)$Se_2$ thus obtained were consistent with that reported in JCPDS number 35-1102, confirming that all samples were pure Cu(In,Ga)$Se_2$ films following selenization at 500°C for 0.5 h. The inset in Figure 2 plots the variation in the XRD intensity ratio of the (112) peak to the (220/204) peak ($I_{(112)}/I_{(220/204)}$) versus the selenization temperature used in the synthesis of the seeding layers. The $I_{(112)}/I_{(220/204)}$ ratio increased with the selenization temperatures of the seeding layers and decreased following selenization at 500°C for the seeding layers. The orientation of $In_2Se_3$ films that were used as the seeding layers greatly affected the orientation of Cu(In,Ga)$Se_2$.

Grazing incidence XRD (GIXRD) with a fixed incident angle ($\omega$) of 7° was used to examine the phases formed in the inner layer of the prepared Cu(In,Ga)$Se_2$ films. Figure 3 displays the GIXRD results of the films that were produced using the seeding layers selenized at various temperatures. The monophasic Cu(In,Ga)$Se_2$ phase was obtained in all of the films without the detection of impurities. The relation between the ratio of the XRD intensity of the (112) peak to the (220/204) peak and the selenization temperatures of the seeding layers was also estimated and was shown in the inset in Figure 3. The above results imply that $I_{(112)}/I_{(220/204)}$ in the interior of Cu(In,Ga)$Se_2$ films varied in a manner similar to that of the surface of Cu(In,Ga)$Se_2$ films as presented in the inset in Figure 2.

The above phenomenon arose from the crystalline symmetry between $In_2Se_3$ and Cu(In,Ga)$Se_2$. According to the literature [13], a crystal symmetry exists between the (006)-oriented $In_2Se_3$ and the (112)-oriented Cu(In,Ga)$Se_2$. In contrast, a crystal symmetry exists between the (300)-oriented $In_2Se_3$ and the (220/204)-oriented Cu(In,Ga)$Se_2$. Hence, the

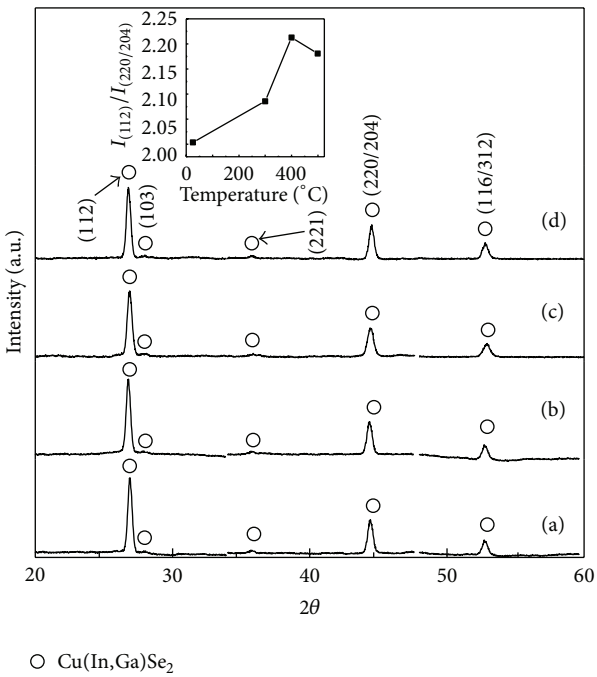


Figure 2: X-ray diffraction patterns of $Cu(In,Ga)Se_2$ films employing the seeding layers (a) without selenization and selenized at (b) 300°C, (c) 400°C, and (d) 500°C. The inset refers to the relation between the intensity ratio of the (112) peak to the (220/204) peak and the seeding layers that were selenized at varied temperatures.

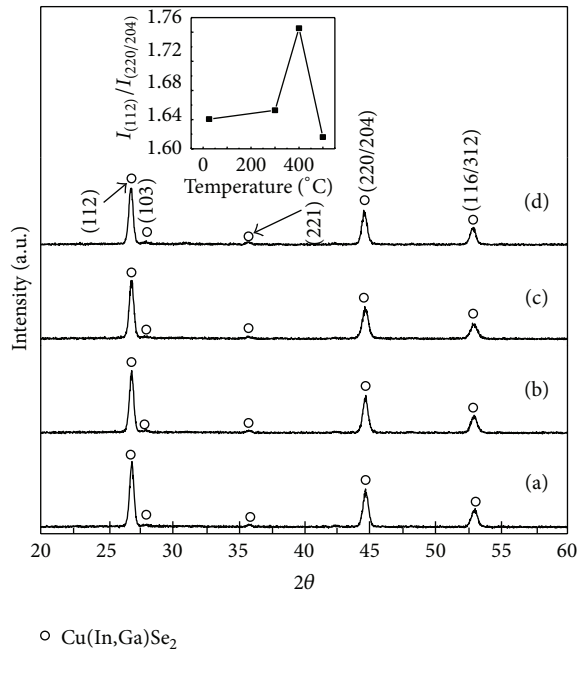


Figure 3: Grazing incident X-ray diffraction patterns of $Cu(In,Ga)Se_2$ films employing the seeding layers (a) without selenization and selenized at (b) 300°C, (c) 400°C, and (d) 500°C as the incident angles were set to 7°. The inset refers to the relation between the intensity ratio of the (112) peak to the (220/204) peak and the seeding layers that were selenized at varied temperatures.

use of the preferred (006)-oriented $In_2Se_3$ as the seeding layer can produce the preferred (112)-orientated $Cu(In,Ga)Se_2$. The preferred (220/204)-orientated $Cu(In,Ga)Se_2$ is obtained using the preferred (330)-oriented $In_2Se_3$ as the seeding layer.

Figure 4 shows the SEM images of the microstructures of the selenized $Cu(In,Ga)Se_2$ films. The inset in Figure 4 displays the cross-sectional micrographs of these films. As shown in Figure 4(a), the microstructure of the films that were prepared using the seeding layer without selenization was porous. Figure 1(a) indicates that these films contained $In_2O_3$. During the selenization process, the oxygen species are evaporated, forming pores in the films. The morphology of $Cu(In,Ga)Se_2$ films thus became increasingly densified as the selenization temperatures of the seeding layers increased (Figures 4(b) and 4(c)). However, as shown in the inset in Figure 4(d), the use of the seeding layer that was selenized at 500°C caused the morphology of $Cu(In,Ga)Se_2$ film to become irregular. The variation of the morphology of the prepared films was caused by the different orientations of the films.

Reportedly, the (112) planes in $Cu(In,Ga)Se_2$ have a lower surface energy than the (220/204) planes [14, 15]. The difference between these surface energies is responsible for the difference between sintering effects of the second phase ($Cu_{2-x}Se$) that is formed during selenization [16]. The fluxing agent of $Cu_{2-x}Se$ phase can easily promote the densification of the (112)-oriented $Cu(In,Ga)Se_2$ films at elevated temperatures. However, the (220/204)-oriented $Cu(In,Ga)Se_2$ with the relatively high surface energy would result in the irregular morphology of the films.

Figure 5 presents the carrier concentration and the resistivity of the prepared $Cu(In,Ga)Se_2$ films. All $Cu(In,Ga)Se_2$ films exhibited p-type conductivity. Their resistivity was decreased and their carrier concentration increased with increasing the selenization temperatures of the seeding layers. The use of the 500°C-selenized $In_2Se_3$ as the seeding layer caused the carrier concentration to decrease and the resistivity to be increased. The resistivity of $Cu(In,Ga)Se_2$ films with the preferred (112) orientation was lower than that of $Cu(In,Ga)Se_2$ films with the preferred (220/204) orientation [17]. The following equation provides the relationship between the resistivity and the carrier concentration [18]:

$$\frac{1}{\rho} = e\left(\mu_n \times n + \mu_p \times p\right), \tag{1}$$

where $\rho$ is the resistivity and $\mu_n$, $\mu_p$, $n$, and $p$ are the electron and hole motilities, and the electron and hole concentrations, respectively. For $p$-type $Cu(In,Ga)Se_2$ films, the product of $\mu_p \times p$ is significant. According to (1), a decrease in the resistivity of $Cu(In,Ga)Se_2$ increases the carrier concentration of the films. In contrast, an increase in the resistivity of the (220/204)-oriented $Cu(In,Ga)Se_2$ reduces the carrier concentration.

Figure 6 plots the $J$-$V$ curves for $Cu(In,Ga)Se_2$ solar cells using the seeding layers that were selenized at different temperatures. Table 1 presents the photovoltaic parameters. The conversion efficiency ($\eta$) increased with the selenization temperature of the seeding layers. The efficiency reached 7.0%

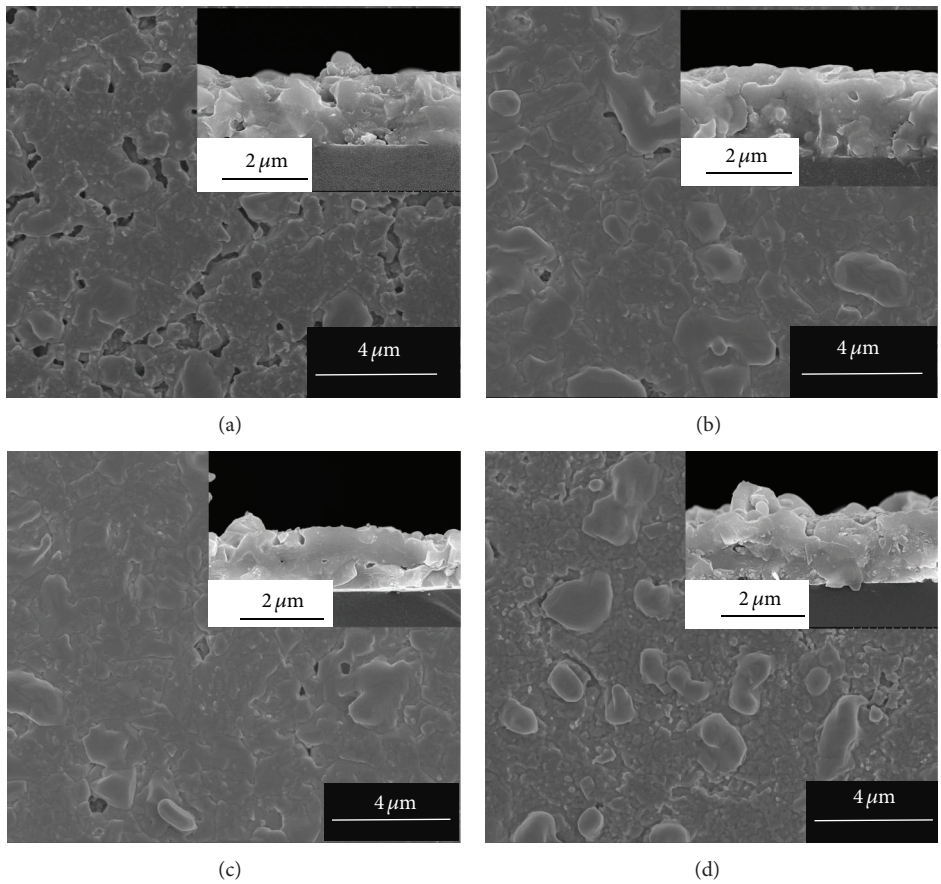


FIGURE 4: Scanning electron micrographs of Cu(In,Ga)$Se_2$ films employing the seeding layers (a) without selenization and selenized at (b) 300°C, (c) 400°C, and (d) 500°C. Insets refer to the cross-section micrographs of the corresponding films.

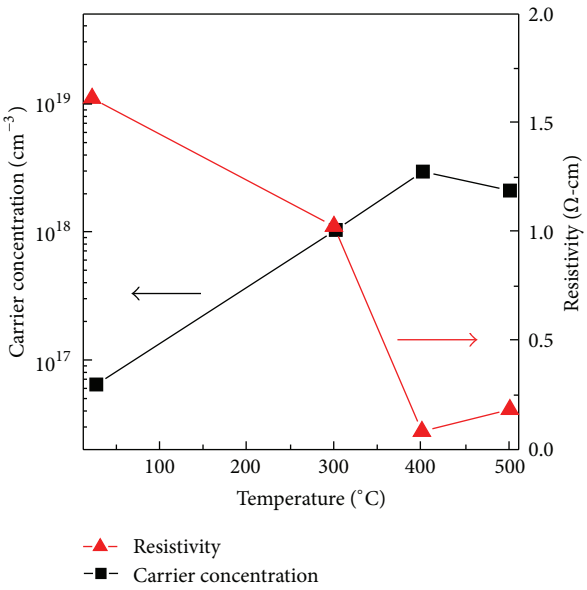


FIGURE 5: Plot of carrier concentration ($N_p$) and resistivity ($\rho$) of Cu(In,Ga)$Se_2$ films employing the seeding layers that were selenized at varied temperatures.

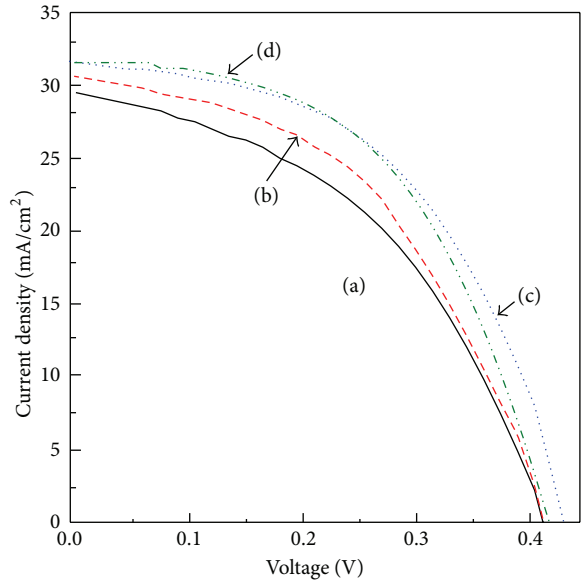


FIGURE 6: Current-voltage characteristics of the fabricated Cu(In, Ga)$Se_2$ solar cells employing the seeding layers (a) without selenization and selenized at (b) 300°C, (c) 400°C, and (d) 500°C.

Table 1: Solar cell parameters of $Cu(In,Ga)Se_2$ films employing the seeding layers (a) without selenization and selenized at (b) 300°C, (c) 400°C, and (d) 500°C.

| | $V_{oc}$ (V) | $J_{sc}$ (mA/cm$^2$) | FF (%) | $\eta$ (%) |
|---|---|---|---|---|
| (a) | 0.41 | 29.6 | 44.9 | 5.6 |
| (b) | 0.42 | 30.0 | 47.5 | 6.1 |
| (c) | 0.44 | 31.6 | 50.8 | 7.0 |
| (d) | 0.42 | 31.6 | 50.3 | 6.8 |

for $Cu(In,Ga)Se_2$ solar cells using the seeding layers that were selenized at 400°C. From Table 1, all samples had the similar short-circuit density ($J_{sc}$). However, the fill factor (FF) increased with the selenization temperatures of the seeding layers because reducing the resistivity of $Cu(In,Ga)Se_2$ film could effectively reduce the series resistance of the solar device, improving the fill factor of the cell. Additionally, the use of the 400°C-selenized $In_2Se_3$ seeding layer increased the open-circuit voltage ($V_{oc}$). The equation that relates the variation of $V_{oc}$ to the carrier concentration ($N_P$) in the absorber layer can be described as the follows [19]:

$$\Delta V_{oc} = \left(\frac{2kT}{q}\right) \ln\left(\sqrt{\frac{N_{P2}}{N_{P1}}}\right), \quad (2)$$

where $\Delta V_{oc}$ is the variation of $V_{oc}$, $k$ is the Boltzmann constant, $T$ represents the temperature in Kelvin, $q$ is the charge of an electron, and $N_P$ is the carrier concentration. Equation (2) is based on the assumption that tunneling mechanism and surface recombination are ignored. According to (2), an increase in $N_{P2}/N_{P1}$ in the absorber layer leads to an increase in $\Delta V_{oc}$, resulting in an increase in $V_{oc}$. Moreover, $Cu(In,Ga)Se_2$ films with the (112) preferential orientation can reportedly be lattice matched with the buffer layers in the fabrication of solar cells [20, 21], yielding a favorable contact between the p-type $Cu(In,Ga)Se_2$ and the n-type buffer layers. Hence, $V_{oc}$ can be significantly increased using $Cu(In,Ga)Se_2$ films with the preferred (112) orientation.

Nevertheless, the (220/204)-oriented films were associated with poorer solar performance because an increase in the resistivity of the films increased the series resistance, causing the reduction of FF. According to the SEM photographs (Figure 4), the rough microstructure and irregular grains of the films could cause the insufficient coverage of CdS buffer layer. The discontinuous covered $Cu(In,Ga)Se_2$ surface is possibly damaged by the ion bombardment during the deposition of i-ZnO window layers in the sputtering process, and the defects will be formed [22]. These defects will form the shunt paths and capture the photogenerated electrons, thereby facilitating the surface recombination of the CIGS/CdS interfaces and resulting in the degradation of the cell performance.

To further investigate the seeding effects from $In_2Se_3$, the PL spectra of the fabricated $Cu(In,Ga)Se_2$ films without seeding layers and with the seeding layer selenized at 400°C are illustrated in Figure 7. It was found that $Cu(In,Ga)Se_2$ films having the seeding layers exhibited much stronger PL intensity than that without seeding layers. It was reported that the defects on $Cu(In,Ga)Se_2$ surface caused surface electron-hole recombination and reduced the PL intensity [23]. These results indicated that the seeding effects from $In_2Se_3$ could effectively reduce the surface recombination of CIGS films, thereby increasing the PL intensity. These results revealed that the electrical properties of $Cu(In,Ga)Se_2$ films can be improved by using oriented $In_2Se_3$ as seeding layers.

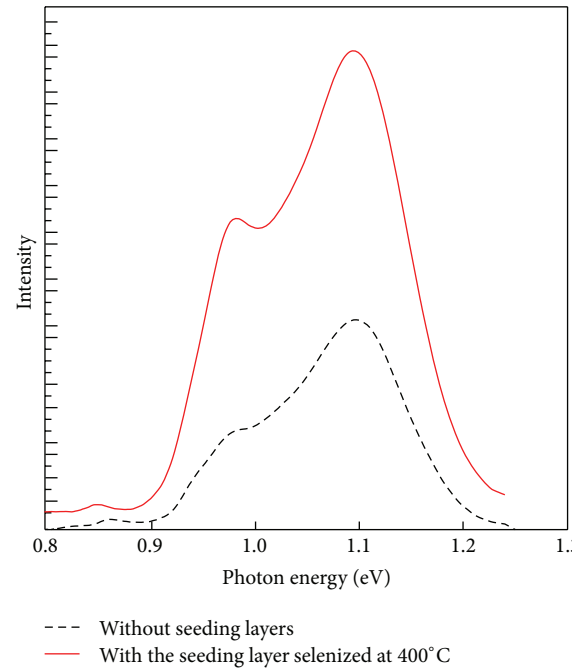


Figure 7: PL spectra of the fabricated $Cu(In,Ga)Se_2$ films without seeding layers and with the seeding layer selenized at 400°C.

## 4. Conclusions

In this study, $In_2Se_3$ seeding layers were utilized to control the orientation of $Cu(In,Ga)Se_2$ films. The hexagonal $\gamma$-$In_2Se_3$ with the preferred (006) orientation was obtained when the indium-containing precursors were selenized at 400°C. The preferred (300)-oriented $\gamma$-$In_2Se_3$ was obtained upon selenization at 500°C. The use of the (006)-oriented $In_2Se_3$ seeding layers resulted in the formation of the (112)-oriented $Cu(In,Ga)Se_2$ films. These films exhibited densified morphologies and improved electrical properties. The (204/220)-oriented $Cu(In,Ga)Se_2$ films were formed when the (300)-oriented $In_2Se_3$ seeding layers were used. The use of the preferred (112)-oriented $Cu(In,Ga)Se_2$ absorber layers increased the conversion efficiency of the solar device to 7.0%.

## Conflict of Interests

The authors declare that there is no conflict of interests regarding the publication of this paper.

## Acknowledgment

The authors would like to thank the National Science Council of China, Taiwan, for partial financial support of this study under Contract no. MOST 102-3113-E-002-012.

## References

[1] F.-S. Chen, C.-H. Wu, and C.-H. Lu, "Low-temperature synthesis of Cu(In,Ga)$Se_2$ thin films using selenium-containing precursors," *International Journal of Applied Ceramic Technology*, vol. 9, no. 4, pp. 853–860, 2012.

[2] C.-H. Wu, F.-S. Chen, S.-H. Lin, and C.-H. Lu, "Preparation and characterization of $CuInSe_2$ particles via the hydrothermal route for thin-film solar cells," *Journal of Alloys and Compounds*, vol. 509, no. 19, pp. 5783–5788, 2011.

[3] T. Mise and T. Nakada, "Microstructural properties of (In, $Ga)_2Se_3$ precursor layers for efficient CIGS thin-film solar cells," *Solar Energy Materials and Solar Cells*, vol. 93, pp. 1000–1003, 2009.

[4] S. Seyrling, A. Chirila, D. Güttler, F. Pianezzi, P. Rossbach, and A. N. Tiwari, "Modification of the three-stage evaporation process for CuIn 1-xGaxSe2 absorber deposition," *Thin Solid Films*, vol. 519, no. 21, pp. 7232–7236, 2011.

[5] C. Amory, J. C. Bernède, E. Halgand, and S. Marsillac, "Cu(In, Ga)$Se_2$ films obtained from $\gamma$-$In_2Se_3$ thin film," *Thin Solid Films*, vol. 431-432, pp. 22–25, 2003.

[6] J. P. Ye, T. Yoshida, Y. Nakamura, and O. Nittono, "Realization of giant optical rotatory power for red and infrared light using $III_2VI_3$ compound semiconductor $(Ga_xIn_{1-x})_2Se_3$," *Japanese Journal of Applied Physics*, vol. 35, pp. 4395–4400, 1996.

[7] M. Yudasaka, T. Matsuoka, and K. Nakanishi, "Indium selenide film formation by the double-source evaporation of indium and selenium," *Thin Solid Films*, vol. 146, no. 1, pp. 65–73, 1987.

[8] S. Nishiwaki, T. Satoh, S. Hayashi et al., "Preparation of Cu(In, Ga)$Se_2$ thin films from Cu–Se/In–Ga–Se precursors for high-efficiency solar cells," *Solar Energy Materials and Solar Cells*, vol. 67, no. 1–4, pp. 217–223, 2001.

[9] M. E. Beck, A. Swartzlander-Guest, R. Matson, J. Keane, and R. Noufi, "CuIn(Ga)$Se_2$-based devices via a novel absorber formation process," *Solar Energy Materials and Solar Cells*, vol. 64, no. 2, pp. 135–165, 2000.

[10] A. R. Uhl, Y. E. Romanyuk, and A. N. Tiwari, "Thin film Cu(In, Ga)$Se_2$ solar cells processed from solution pastes with polymethyl methacrylate binder," *Thin Solid Films*, vol. 519, no. 21, pp. 7259–7263, 2011.

[11] C. Amory, J. C. Bernède, and S. Marsillac, "Study of a growth instability of $\lambda$-In2Se3," *Journal of Applied Physics*, vol. 94, no. 10, pp. 6945–6948, 2003.

[12] M. A. Contreras, B. Egaas, D. King, A. Swartzlander, and T. Dullweber, "Texture manipulation of $CuInSe_2$ thin films," *Thin Solid Films*, vol. 361–362, pp. 167–171, 2000.

[13] J. C. Bernède, S. Marsillac, A. Conan, and A. Godoy, "The influence of microcrystalline inhomogeneities embedded in amorphous $In_xSe_{100-x}$ films on their electrical and optical properties," *Journal of Physics: Condensed Matter*, vol. 8, no. 19, pp. 3439–3451, 1996.

[14] O. Lundberg, M. Bodegård, and L. Stolt, "Rapid growth of thin Cu(In,Ga)Se2 layers for solar cells," *Thin Solid Films*, vol. 431-432, pp. 26–30, 2003.

[15] D. Liao and A. Rockett, "Epitaxial growth of Cu(In,Ga)$Se_2$ on GaAs(110)," *Journal of Applied Physics*, vol. 91, no. 3, pp. 1978–1983, 2002.

[16] K. H. Kim, K. H. Yoon, J. H. Yun, and B. T. Ahn, "Effects of Se flux on the microstructure of Cu(In,Ga)$Se_2$ thin film deposited by a three-stage co-evaporation process," *Electrochemical and Solid-State Letters*, vol. 9, no. 8, pp. A382–A385, 2006.

[17] M. A. Contreras, K. M. Jones, L. Gedvilas, and R. Matson, "Preferred orientation in polycrystalline Cu(In,Ga)$Se_2$ and its effect on absorber thin-films and device," in *Proceedings of the 16th European Photovoltaic Solar Energy Conference and Exhibition*, pp. 732–735, Glasgow, UK, 2000.

[18] O. Bamiduro, G. Chennamadhava, R. Mundle et al., "Synthesis and characterization of one-step electrodeposited CuIn(1-x)GaxSe2/Mo/glass films at atmospheric conditions," *Solar Energy*, vol. 85, no. 3, pp. 545–552, 2011.

[19] M. Ruckh, D. Schmid, M. Kaise, R. Schäffler, T. Walter, and H. W. Schock, "Influence of substrates on the electrical properties of Cu(In,Ga)$Se_2$ thin films," in *Proceedings of the Conference Record of the IEEE 1st World Conference on Photovoltaic Energy Conversion*, pp. 156–159, 1994.

[20] A. Gupta and S. Isomura, "Precursor modification for preparation of CIS films by selenization technique," *Solar Energy Materials and Solar Cells*, vol. 53, no. 3-4, pp. 385–401, 1998.

[21] J. López-García and C. Guillén, "Adjustment of the selenium amount provided during formation of $CuInSe_2$ thin films from the metallic precursors," *Physica Status Solidi A*, vol. 206, no. 1, pp. 84–90, 2009.

[22] T. Nakada, K. Furumi, and A. Kunioka, "High-efficiency cadmium-free Cu(In,Ga)$Se_2$ thin-film solar cells with chemically deposited ZnS buffer layers," *IEEE Transactions on Electron Devices*, vol. 46, no. 10, pp. 2093–2097, 1999.

[23] S. Shirakata and T. Nakada, "Time-resolved photoluminescence in Cu(In,Ga)$Se_2$ thin films and solar cells," *Thin Solid Films*, vol. 515, no. 15, pp. 6151–6154, 2007.

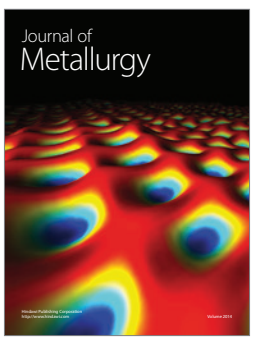

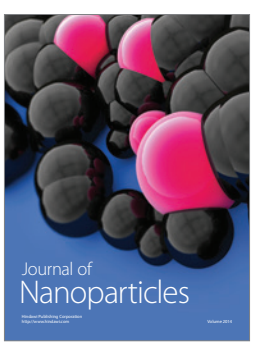

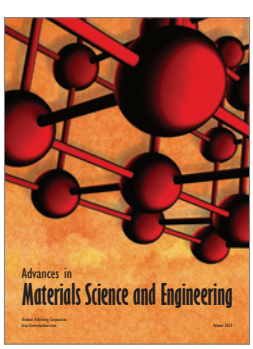

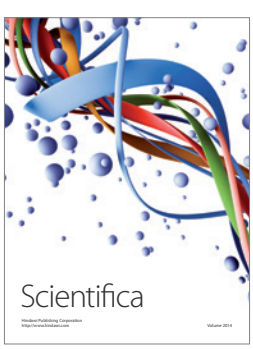

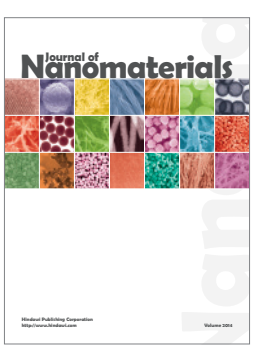

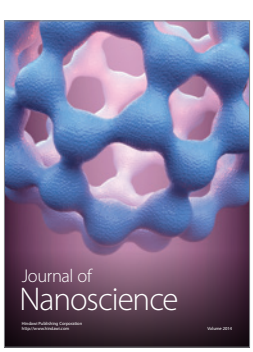

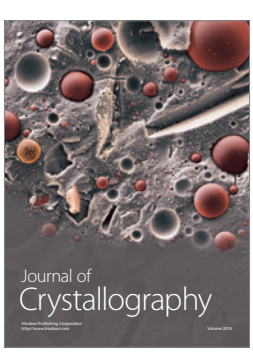

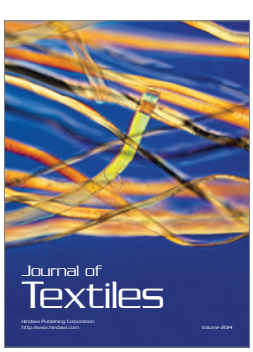


Hindawi

Submit your manuscripts at
http://www.hindawi.com